

Complete Fault Rock Distribution Analysis along the Hirabayashi NIED Core Penetrating the Nojima Fault at 1,140m Depth, Awaji Island, Southwest Japan

By

Hidemi TANAKA^{*1}, Tatsuo MATSUDA^{*2}, Kentaro OMURA^{*2},
Ryuji IKEDA^{*2}, Kenta KOBAYASHI^{*3}, Koji SHIMADA^{*4},
Takashi ARAI^{*5}, Tomoaki TOMITA^{*6}, and Satoshi HIRANO^{*7}

^{*1}Ehime University, Ehime, tanaka@sci.ehime-u.ac.jp

^{*2}National Research Institute for Earth Science and Disaster Prevention Japan,
mtatsuo@bosai.go.jp, omura@bosai.go.jp, ikeda@bosai.go.jp

^{*3}Niigata University, Niigata, kenkoba@gs.niigata-u.ac.jp

^{*4}Waseda University, Tokyo, 698g5040@mn.waseda.ac.jp

^{*5}Shinshu University, Nagano, sa96401@gipac.shinshu-u.ac.jp

^{*6}Tsukuba University, Ibaraki, tomita@luna.riko.tsukuba.ac.jp

^{*7}Japan Marine Science and Technology Center, Kanagawa, hiranos@jamstec.go.jp

Abstract

The distribution and petrological characteristics of fault rocks in a shallow fault zone (1,140m depth) of granitic origin were examined in a fault zone in the NIED (the National Research Institute for Earth Science and Disaster Prevention) drill core (NIED core) penetrating the Nojima fault, which was activated during the 1995 Hyogo-ken Nanbu Earthquake ($M=7.2$). The NIED core consists of granodiorite and porphyritic intrusive rocks including a Nojima fault zone which involves six thin shear zones (A to F zones). These shear zones are generally surrounded by fault related rocks that are less pulverized and less altered (WPAR). The fault zone architecture is clarified as follows : (1) The total thickness of the Nojima fault zone at a depth of 1,140m is close to, but thicker than Ca. 70m. (2) All shear zones were evolved from the WPAR, indicating that pulverization and alteration of recent activity were more diffused at the initial stage of faulting, becoming gradually localized to individual shear zones. (3) Centralized layers of the shear zones contain ultracataclasite, and the D shear zone contains pseudotachylite, indicating that shear zones A to F can be regarded as a high velocity frictional zone, centralized by D zone. (4) The hanging wall and footwall of each shear zone typically shows explosion brecciation texture with carbonate and zeolite matrices, respectively, which are also regarded as dilatant co-seismic shear zones. It is possible that these zones function as a trap zone for fluid or gas during post-/interseismic periods. (5) The thick foliated clay gouge zone, which is one of the typical fault rocks in a shallow fault zone, was not detected at the 1,140m fault zone in the NIED core.

Key words : Hyogo-ken Nanbu earthquake, Nojima fault, Fault rock distribution, Microstructure, Deformation, Alteration

1. Introduction

At 5: 46 AM, on the January 17, 1995, an $M=7.2$ earthquake struck the southern part of Kobe city and the northwestern part of Awaji island (Hyogo-ken Nanbu earthquake). The epicenter was located at the Akashi straight and the focal depth was reported to be 14km. Surface rupture appeared more than 10 km

long along the preexisting NE-SW striking Nojima fault (Awata *et al.*, 1996). Maximum displacement of surface rupture was observed at Nojima-Hirabayashi located at the northern part as 180cm right lateral and 130cm reverse components (Nakata *et al.*, 1995; Awata *et al.*, 1996). In 1995, the National Research Institute for Earth Science and Disaster Prevention

(NIED) began a drilling project to explore the natural state of the fault zone just after the big earthquake at Nojima Hirabayashi, and successfully penetrated the fault zone recovering the drill core of some 800m in length (1,000 to 1,800m depths) containing almost complete fault rocks from across the fault zones. The drill core is referred to as NIED core in this paper.

Fault rock distribution is one of the most important issues in understanding the dynamics of the fault zone during seismic cycles (Tanaka and Itaya, 1998). However, previous studies of the natural fault rocks in a brittle regime, from the seismogenic depth to the surface have been limited for the following two reasons, (1) processing the brittle fault rocks can be problematic since they are generally very soft and fragile, and (2) outcrop observation is limited because they are easily eroded and if present, they are usually modified mechanically and chemically by weathering in a surface condition. The NIED core contains not only fault rocks that have experienced a big earthquake but also a perfect succession from host rock to fault rocks all of which have never been weathered by surface conditions. The Cajon Pass Project is well known as a fault related drilling project (Zoback *et al.*, 1988). The main purpose of this project was to investigate the geothermal anomaly along the San Andreas Fault, and drilling was performed about 4km northeast of the San Andreas Fault trace (Zoback and Lachenbruch, 1992). Therefore, detailed geological examinations of the NIED core are worthwhile for a better understanding of the fault zone architecture at shallow depths of the granitic crust. In the first instance, we have attempted to conduct a detailed analysis of fault rock distribution, and of the characterization of deformation/alteration microscopic textures.

3. Outline of geology along the Nojima surface rupture and drill core

The Nojima fault is an 8km long right-lateral active fault with a minor reverse component (The research group for active faults of Japan, 1991). This fault runs along the northwestern margin of Awaji Island (Fig. 1), trending northeast and dipping south-eastwards at a high angle (Mizuno *et al.*, 1990). The fault juxtaposes Cretaceous granitic rocks (Nojima Granodiorite, 66 to 88 Ma; Takahashi, 1992) partly overlain by Neogene and Quaternary sediments on the southeastern side with Neogene and Quaternary sediments on the northwestern side. The sediments on both sides belong to the middle Miocene Kobe Group and Plio-Pleistocene Osaka Group. These groups are

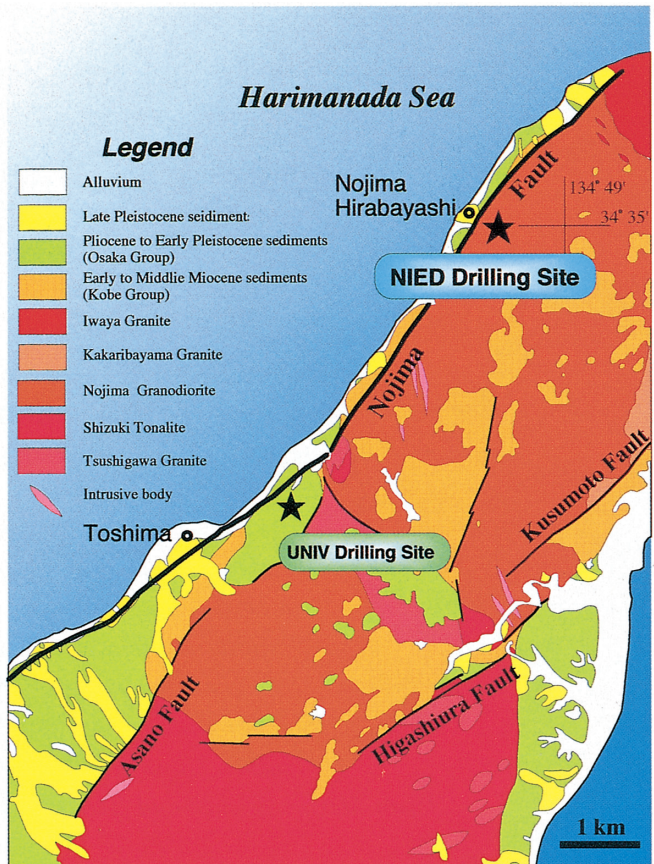


Fig. 1 Geological map around the northwestern part of Awaji Island. The NIED drilling site is located at Nojima Hirabayashi, along the northern part of Nojima fault. The drilling site of the University group is also shown on this map.

composed mainly of sand and gravel beds intercalated with thin layers of mud (Mizuno *et al.*, 1990).

The surface rupture was basically generated along the Nojima fault but extended farther southwest. The total length was estimated as 10km (Awata *et al.*, 1996) to 18km (Lin and Uda, 1996). The southwestern part of the surface rupture deviated from the Nojima fault to the west and extended into Neogene sediments (Awata *et al.*, 1996). The NIED drilling site was located about 300m southeast of the surface rupture of the Nojima fault near Nojima-Hirabayashi (Fig. 1). Drilling was performed down to a depth of 1,822m along the direction of the drilling, with an average inclination of about 88 degrees to the northwest. It succeeded in penetrating and recovering the drill core containing the surface of the Nojima fault at drilling depths of 1,140m, 1,300m and 1,750m, respectively (see Ikeda *et al.*, 2001). The dip of the Nojima fault is inferred to be Ca. 60°degrees at 1,140m depth from a spatial relationship among the outcrop of surface rupture, the depth of the fault surface in the GSJ drilling hole and the 1,140m fault surface of the

NIED drill hole and the dip of the fault surface in the drill core. The 1,140m fault zone of the NIED core mainly consists of Nojima granodiorite accompanied by minor porphyry intrusions. The fault rocks are distributed at depths extending from about 1,000 to 1,200m, and detailed examinations of fault rock distribution were performed at depths ranging from 1,054.00 to 1,189.55m, as described below. Several shear zones exist in a fault zone and each shear zone is relatively narrow and surrounded by fault related rocks that are less deformed and altered, and that are distributed over a wide area. This type of fault rock is referred to as weakly-pulverized and altered rock (WPAR) in this paper (Tanaka *et al.*, 1999).

3. Fault rock distribution along the 1,140m fault zone of the NIED core

3.1 Analytical methods

Repeated failures during core processing led us to develop the method outlined in Tanaka *et al.*, (2000). The method was applied to depths extending from 1,054.00m to 1,189.55m, where most of the core was composed of soft and fragile fault rocks.

Basically, each core piece was carved into three parts. Figure 2 shows the method of carving the core pieces into AH (Archive Half) and WH (Working Half) and further carving AH into AA (for Analyzing) and AS (Slab for preservation). After carving, the carved surface was fixed again using resin. AA was

utilized mainly for chemical composition and crystal structure analysis, AS for texture observations and non-destructive measurements/analysis (such as color analysis) and long term preservation after the surfaces had been polished, and WH for various kinds of measurements/observations and analysis requiring large volumes of the core.

In order to understand the whole trend of fault rock distribution in the NIED core, the surfaces of the entire drill core (1,054.00 to 1,189.55m) were first observed visually and a rough fault rock distribution map was prepared. After completion of core processing, fault rock distribution was re-examined via an observation of some 1,300 pieces of the polished slabs (AS). Then, 134 thin sections were prepared throughout the core for observation of deformation/alteration microstructures. The results of the detailed description are shown in the Appendix. The rock types in the drill core were categorized into the following six types : (1) granodiorite (host rock), (2) altered porphyry intrusive rocks, (3) weakly pulverized and altered fault-related rocks (WPAR), (4) fault breccia, (5) ultracataclasite, and (6) pseudotachylite. Categories (3) to (6) correspond to the fault rock classification of Higgins (1971) and Sibson (1977) that was partly modified by Chester *et al.* (1993). The original fault rock distribution map was revised to create a precise fault rock distribution map.

3.2 Petrological characteristics of host and fault rocks from the NIED drill hole

3.2.1 Granodiorite (host rock)

The occurrence and texture of Nojima granodiorite was in detail described by Mizuno *et al.* (1990). The mesoscopic textural characteristics are as follows (Fig. 3a). Short, column-shaped hornblende crystals and thin crystals of biotite are scattered in larger quartz and feldspar crystals. Feldspars are milky white in color and quartz is relatively clear. Xenoliths, several centimeters in diameter, are occasionally included. The xenoliths have a relatively dark color, possibly due to a greater abundance of mafic minerals. Biotite K-Ar ages were reported to be 81 Ma for this rock (Takahashi, 1992). In the drilled core, although some feldspar grains had altered to become an orange color, few other alteration or deformation features were observed on the polished surfaces.

Under the microscope, the host rock shows some intercrystalline cracks containing carbonate and zeolite minerals, although their density is quite low and they are usually very narrow (Fig. 4a). Coexisting euhedral zeolite and carbonate minerals are occasionally observed in these veins. Rare micro shear

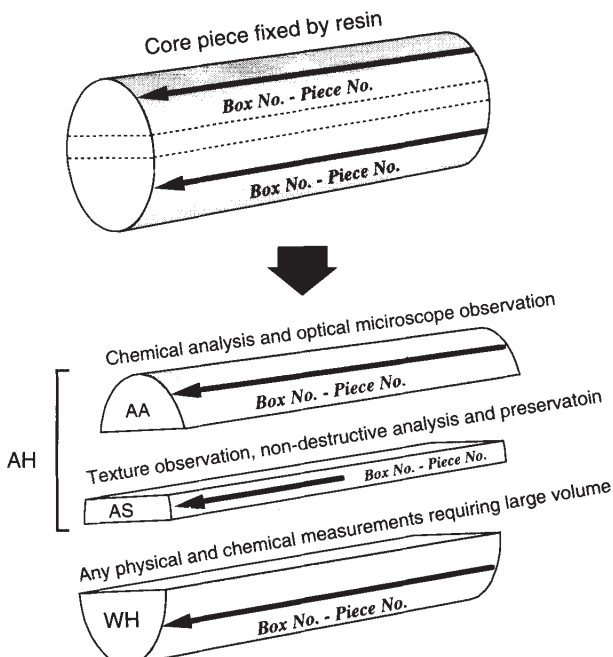


Fig. 2 The method of carving a core piece into three slabs, AA, AS, and WH. See text for detailed explanation.

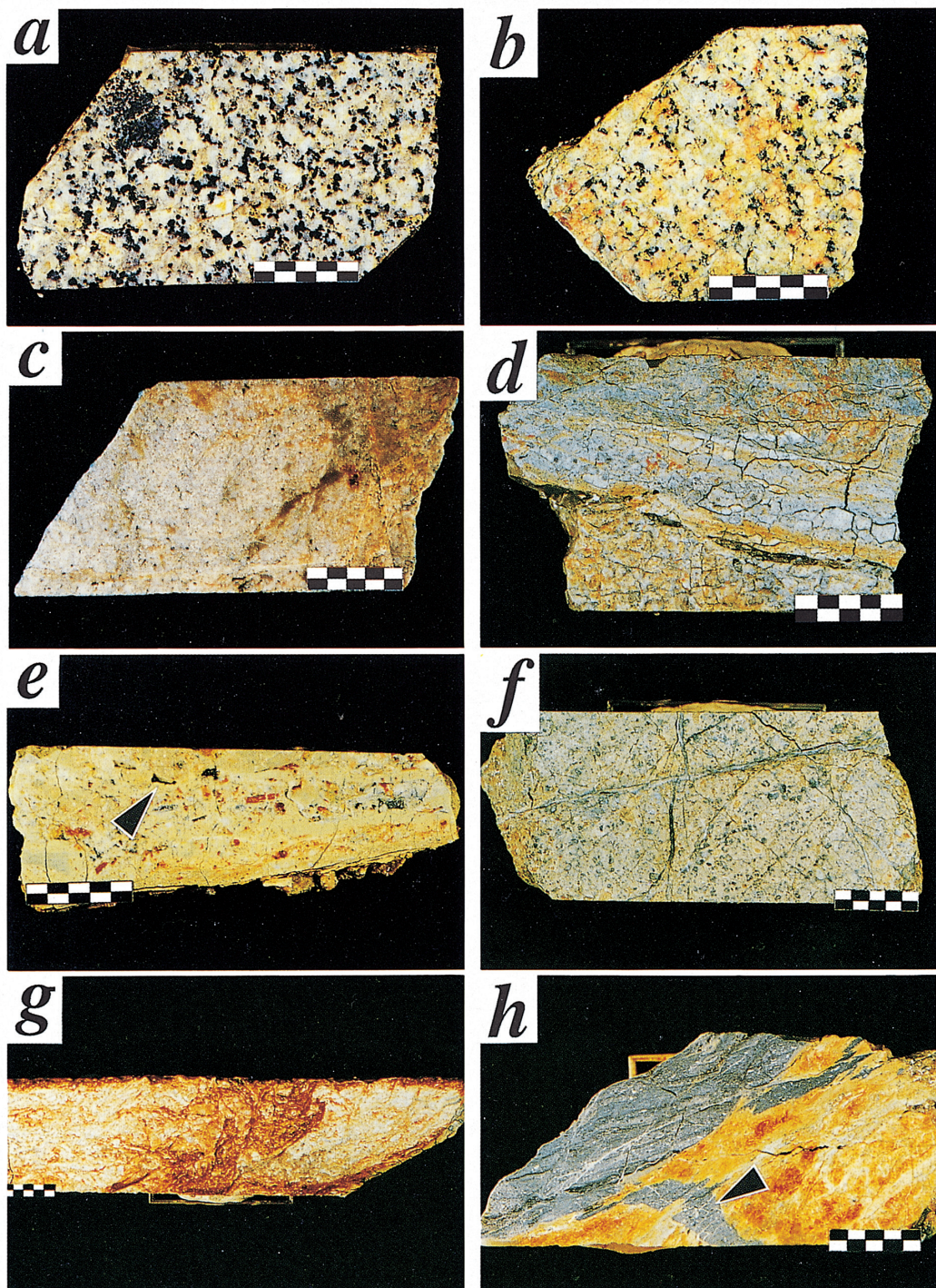


Fig. 3 Photographs showing mesoscopic textures observed on the polished surfaces of AS of each type of host and fault rocks. Bar scale : 1 cm for a couple of thick white and black bars.
a, Granodiorite (host rock ; 54-32 : 1,178.26 to 1,178.35m depth) showing a "fresh" occurrence in the 1,140 m depth fault zone. b, Weakly pulverized and altered fault-related rock (WPAR ; 39-18 : 1,104.90 to 1,104.99m). Typical occurrence of the WPAR with carbonate alteration. c, Typical occurrence of the WPAR with zeolite alteration (46-25 : 1,145.75 to 1,145.83m). d, Ultracataclasite (44-26-1 : 1,135.12 to 1,135.25m). e, Ultracataclasite (39-13 : 1,103.90 to 1,104.00m). Hydraulic brecciation texture with carbonate matrix. Note the visible pores (black arrow) present in the matrix. f, Porphyry intrusive rock (44-11-2 : 1,133.00 to 1,133.24m). g, Foliated ultracataclasite (45-25-2 : 1,140.72 to 1,140.96m). h, Pseudotachylite (45-24-1 : 1,140.57 to 1,140.66m). An arrow indicates an injection vein of pseudotachylite into the adjacent ultracataclasite layer.

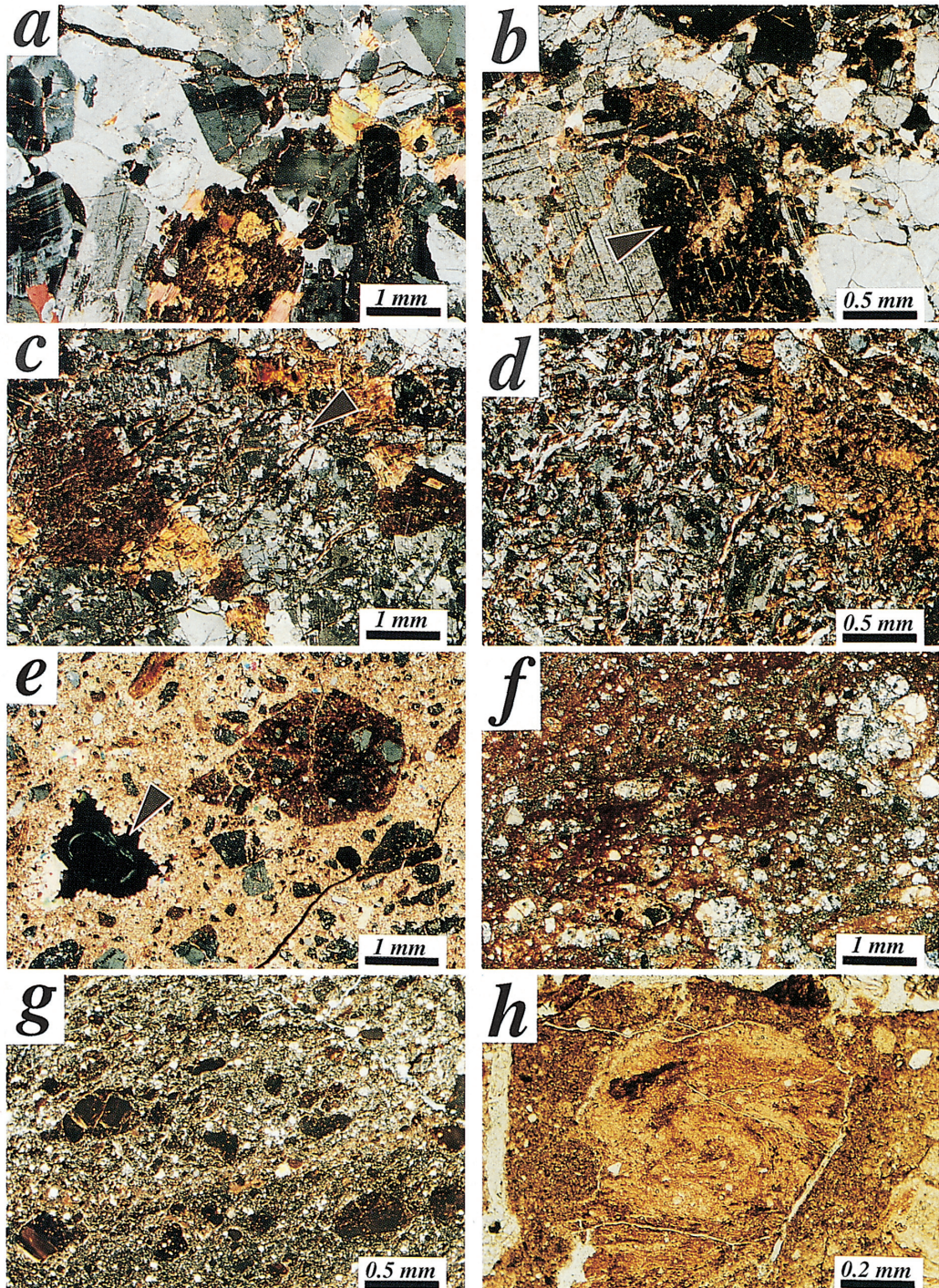


Fig. 4 Photographs showing microscopic textures observed in the thin sections of each type of host and fault rocks. a, Granodiorite (54-32 : 1,178.26 to 1,178.35m depth). Hornblende crystal (bottom center of the photograph) is partly replaced by mafic carbonate minerals and biotite. b, WPAR with carbonate alteration (42-4-1 : 1,122.29 to 1,122.43m). Note that center portion of plagioclase is partly replaced by carbonates (black arrow). c, WPAR with zeolite alteration (39-18 : 1,104.90 to 1,104.99m). Note that plagioclase is mostly replaced by zeolites (black arrow). d, Fault breccia originated from porphyry intrusive rock. Small, lath shape crystals of plagioclase remain in the sheared matrix (43-16 : 1,128.32 to 1,128.37m). e, Ultracataclasite showing hydraulic brecciation texture with carbonate matrix (39-13 : 1,103.90 to 1,104.00m). Larger crystals of calcite surround a pore, indicating that CO₂ rich fluid was filled in the pore. f, Foliated ultracataclasite with precipitation of iron hydroxide minerals (45-25-2 : 1,140.72 to 1,140.96m). g, Dark, opaque pseudotachylite grains involved in the matrix of ultracataclasite (45-24-1 : 1,140.57 to 1,140.66m). This type of fault rocks is referred to as pseudotachylite in this paper. h, A pseudotachylite clast in a vein filled with crushed, ultrafine material within ultracataclasite (45-19B : 1,140.03 to 1,140.16m). A spiral texture, presumably formed by turbulent flow, is preserved in the clast.

zones contain a matrix of crushed grains of the host granodiorite and carbonate micro grains and clasts of quartz, feldspars, zeolites and carbonate minerals. Wavy and blocky extinction and healed intra-grain cracks are commonly observed in quartz grains. Feldspar grains are less deformed than quartz, but occasionally weak wavy extinction of the feldspars can be observed. However, core portions of plagioclase crystals are commonly replaced by micro grains of carbonate, zeolite and sericite. Some biotite grains are partly altered to chlorite. Carbonate minerals occasionally occur as microlenses along biotite cleavages. Kink bands are well developed in some grains of biotite at large angles to their cleavages. Hornblades are partly altered to carbonate minerals and biotite along their cleavages (Fig. 4a).

3.2.2 Altered porphyry intrusive rocks

Minor porphyry intrusive rocks were observed close to the center zone of the fault (Fig. 5). They are more or less altered and deformed. Phenocrysts varying in color from milky white to light brown are scattered in light brown colored groundmass. Grayish white veins are apparent in the heavily altered part (Fig. 3f). Porphyritic rocks are altered in a similar manner to the fault rocks of granitic origin indicating that porphyry had intruded prior to the recent activity of the Nojima fault.

Under the microscope, the groundmass is composed of plagioclase laths, quartz, biotite and mafic carbonate (Fig. 4d). Phenocrysts are dominated by plagioclase accompanied by quartz, biotite and relict crystals of hornblende. The plagioclase phenocrysts are commonly replaced by fine-grained carbonate and

zeolite minerals especially in the heavily altered portion. Within the most heavily altered part, the groundmass of the porphyry has commonly altered to become cryptocrystalline materials (Fig. 4d). Few mafic minerals are preserved in these porphyritic rocks. All of these textures are commonly cut by carbonate and zeolite veins.

3.2.3 Weakly pulverized and altered fault rocks (WPAR)

The WPAR shows varying degrees of pulverization and alteration. Thus, we tentatively subdivided the WPAR based on the qualitative measure of degrees of pulverization and alteration apparent at the mesoscopic scale (Table 1). General mesoscopic descriptions of WPAR are as follows. Host rock texture is disturbed and mafic minerals are generally reduced both in size and amount due to pulverization and alteration (Fig. 3b, c). The mafic minerals are generally replaced by grayish green to grayish brown colored minerals. The cores of feldspar grains are altered and generally change color becoming grayish white or light orange. The density of the shear surfaces is low, and the shears are generally filled with grayish white, brown and greenish gray materials. The disappearance of mafic minerals and alteration of feldspar grains are common along these shear surfaces.

Intragranular cracks are prominent in quartz grains and are commonly filled with carbonate (calcite and mafic carbonates) and zeolite (laumontite and stilbite) minerals (Fig. 4b, c). Intragranular cracks are less common in feldspar grains, but the filling materials are similar to those in quartz. Intergranular cracks are also prominent features. They are filled with the

Table 1 Criteria for qualitative, visual classification of the WPAR. "Density of shear surfaces" is defined as the area ratio occupied by shear surfaces to the area of the core slab (AS in Fig. 2), and "Contents of residual mafic minerals" is defined as the ratio of mafic mineral contents of the sample to that of the fresh host rock sample.

Pulverization Index (PI)	Density of shear surfaces	Characteristics of cracks and shear surfaces	
0	< 10%	healed cracks	
1	< 30%	carbonate and zeolite veins	
2	< 50%	carbonate, zeolite and clay veins, and/or shear surfaces containing crushed host rock minerals	
Alteration Index (AI)	Contents of residual mafic minerals	Alteration of feldspars	Characteristics of secondary minerals
0	> 70%	-	-
1	> 20%	change in color into light gray, light brown and light orange	Replacement of mafic minerals (spot distribution)
2	> 5%	change in color as same as above + reduction in contents	abundant veins

same minerals as the intragranular cracks, but contain relatively large, euhedral carbonate and zeolite crystals. Micro shear surfaces are abundant and commonly contain clasts of crushed igneous, carbonate and zeolite minerals and a matrix of fine grained quartz, feldspar, carbonate, zeolite and iron hydroxide minerals. They commonly show a random fabric texture. The cores of many feldspar grains are replaced by fine-grained mafic carbonate and zeolite minerals (Fig. 4b, c). Lath shaped crystals (possibly stilpnomelane) occasionally overprint feldspars. A comparison of the alteration of feldspar grains on the polished surfaces with those in thin sections clarifies the fact that the brown or orange colored feldspar on the polished surfaces corresponds to replacement by mafic carbonate minerals and grayish white colored feldspar corresponds to replacement by zeolite minerals. Biotite grains are less abundant and smaller in size than those in the host rocks, mainly due to pulverization and alteration. Mafic carbonate and/or zeolite minerals showing a spindle shape or forming irregular aggregates are deposited between the cleavages of biotite grains. Some biotite grains show complete pseudomorphic replacement by these carbonates. Other examples of deformation and alteration of biotite include (1) kink bands which bend the intra-cleavage carbonate and zeolite minerals and (2) exfoliation brecciation along cleavages to fine grain size, which are commonly incorporated into shear surfaces and cracks. Hornblende crystals also show complete pseudomorphic replacement by biotite and/or cryptocrystalline dark materials (possibly mafic carbonate). These characteristics of pulverization and alteration, including the density of intra-and inter-granular cracks, micro-shear zones, degree of alteration of feldspar grains and mafic minerals become more intense with decreasing distance from the core part of each shear zone (Fig. 5).

3.2.4 Fault breccia

Feldspar grains generally change in color to light brown or light orange and are greatly reduced in abundance. Few mafic minerals are observed in the texture. Anastomosing development of micro shear zones, over 5mm thick, are commonly observed. They contain crushed fragments of host rock minerals surrounded by a matrix of brown-colored alteration products and/or ultrafine crystals of zeolite. The mean size of the clasts is 3mm, and the maximum is more than 50mm. Some clasts are rounded in shape, possibly due to wear and/or dissolution. The texture of the host rock or WPAR is occasionally preserved in the larger clasts. The fault breccia basically shows a

random fabric, but a mesoscopic foliated texture is observed in which the fault breccia adjoins other types of fault rock, such as ultracataclasite or WPAR. Fault breccia is more intensely pulverized and altered with decreasing distance to the ultracataclasite zone.

The texture of the host rock can no longer be observed under the microscope, and the typical texture is one in which larger clasts are surrounded by a finer-grained matrix. The matrix is composed of crushed crystals of quartz and feldspars, mafic carbonate, iron hydroxide, and zeolite minerals. Clasts include quartz, healed aggregates of quartz and feldspars, and carbonate and zeolite minerals. Feldspar grains are heavily altered to carbonate and/or zeolite minerals. The biotite grains are greatly reduced in size and abundance due to comminution and alteration. Hornblendes and their pseudomorphic crystals are no longer observed. Foliation is recognized where iron hydroxide minerals are concentrated, although random fabric is dominant texture. The foliation is cut by veins containing iron hydroxide and mafic carbonate minerals.

3.2.5 Ultracataclasite

The general characteristics of ultracataclasite are well described by Chester and Logan (1986), and Chester *et al.* (1993). The texture of the host rock and most of the minerals derived from the host rock derived are obliterated except those in relatively larger clasts. Instead, ultracataclasite is composed of very fine-grained materials showing various colors such as light grayish brown, light brown and light gray (for example, Fig. 3d, e, g). Small amounts of fine-grained and rounded clasts are scattered in the variably colored matrix. The ultracataclasite is gradually developed by overprinting the fault breccia. However, in some cases, direct contact with the WPAR or fault breccia bounded by shear surfaces is observed. Foliations are commonly recognized by the color banding of these materials (Fig. 3d, g).

The ultracataclasite shows typical “clasts supported by matrix”, random fabric texture (Fig. 4e, f). The matrix is composed of submicron-sized crystals of quartz, zeolites, carbonates, iron hydroxides, and minor quantities of clay minerals. The clasts are composed of crushed quartz, aggregates preserving the texture of hydraulic brecciation, carbonate minerals and zeolites. The clasts are finer and more rounded in shape than those in fault breccia. Most of the feldspars are replaced by carbonate and/or zeolite minerals. Mafic minerals are no longer observed even under high magnifications. Foliations are developed where iron hydroxide minerals are precipitated in

micro shear zones, resulting in the formation of color banding in the ultracataclasite. These textures indicate that micro foliations are formed at the same time or after the precipitation of the iron hydroxide minerals. These textures are further overprinted by a hydraulic brecciation texture in some places (Fig. 4e), especially at the margins of the ultracataclasite zone. The matrix of this breccia is composed of fine-grained carbonate minerals and the clasts are composed of brecciated grains of ultracataclasite itself (Fig. 4e).

3.2.6 Pseudotachylite

Pseudotachylite is found as thin gray colored layers and interspersed with ultracataclasites at a depth of 1,140m in the Nojima fault zone (Fig. 3h). Pseudotachylite, which is referred to here, is tentatively categorized on the basis of the meso-and microscopic characteristics. Few fragments are observed in the pseudotachylite at the mesoscopic scale; thin, dark gray colored materials are intercalated. Foliations are recognized by dark gray/gray color banding and the parallel arrangement of micro fragments. An injection structure of pseudotachylite into ultracataclasite layer is clearly observed (Fig. 3h). The injection structure and the foliations in the pseudotachylite are cut at a low angle by the surface of the boundary shear between the ultracataclasite and the pseudotachylite (Fig. 3h). The foliation developed in the ultracataclasite is also cut by the surfaces of the boundary shear. These observations indicate that the pseudotachylite was generated prior to the ultracataclasite and the newest structure is the boundary shear surface.

The fundamental texture is “clasts supported by matrix” at the microscopic scale (Fig. 4g). The matrix is predominantly composed of cryptocrystalline materials, with very fine-grained quartz and minor quantities of very fine grained carbonates scattered through it. The pseudotachylite does not contain iron hydroxide minerals, which are concentrated in the ultracataclasite. One of the most prominent features of the pseudotachylite in the NIED core is that fragments of pseudotachylite are scattered as clasts or thin layers in the ultrafine grained matrix (Fig. 4g). Wavy foliations are occasionally preserved in these clasts. Spiral / vortex texture is preserved in some of these grains (Fig. 4h). The whole texture of the pseudotachylite is cut by thin and anastomosing shear surfaces containing clay minerals. These facts also indicate the pseudotachylite is older than ultracataclasite.

4. Characterization of alteration of the fault rocks

Most of the alterations to host and fault rocks are basically categorized into the following three types based on the microtextural observations (see Appendix for reference). (1) Carbonate type (C type): Typical meso-/microscopic textures are shown in Fig. 3b and Fig. 4b. The crack fillings are dominated by carbonate minerals. Further, plagioclase crystals are more or less replaced by carbonates. Microspherules of mafic carbonate are commonly observed between the cleavages of biotite. (2) Zeolite type (Z type): Typical textures are shown in Fig. 3c and Fig. 4c. The crack fillings are dominated by zeolite minerals. Plagioclase crystals are replaced by zeolite. Microlenses of zeolite are observed between cleavages of biotite as well as carbonate spherules. Fault rocks with Z type alteration are generally overprinted by C type alteration, which means coexisting types of alteration are commonly observed. This type of alteration is referred to as Carbonate/Zeolite type (C/Z type). (3) Mafic Carbonate/Iron Hydroxide type (MC/IH type): Typical textures are shown in Fig. 3g and Fig. 4e, f. This type of alteration is deeply involved with fault breccia and ultracataclasite. The ultrafine grain size of the mafic carbonate/iron hydroxide minerals serves as the matrix of these fault rocks. Clasts in those fault rocks commonly preserve textures of C, Z and C/Z types. While clasts of ultracataclasite are preserved in a hydraulic brecciation texture with carbonate matrix (Fig. 3e, Fig. 4e), indicating repeated process of brecciation coupled with C and MC/IH types alteration. It should be noted that flow textures are prominent where iron hydroxide minerals are precipitated.

5. Discussion

5.1 Distribution and structural evolution of each shear zone in the Nojima fault

Detailed fault rock distribution is shown in Fig. 5. At the mesoscopic scale of observation, fault related comminution and alteration gradually increase in the NIED core from the top and bottom to the core zone of the Nojima fault (around 1,140m) (Fig. 5). Fresh host rocks are not present even in the shallower and deeper parts in the extent except the depth range of from 1,184.70m to 1,185.27m. Thus, the entire extent from the depth of 1,054.00m to 1,189.55m is treated as the Nojima fault zone in this paper. The fault zone may extend to shallower and greater depths, since pulverization and alteration are observed even at the top and bottom of the analyzed extent. In the Nojima

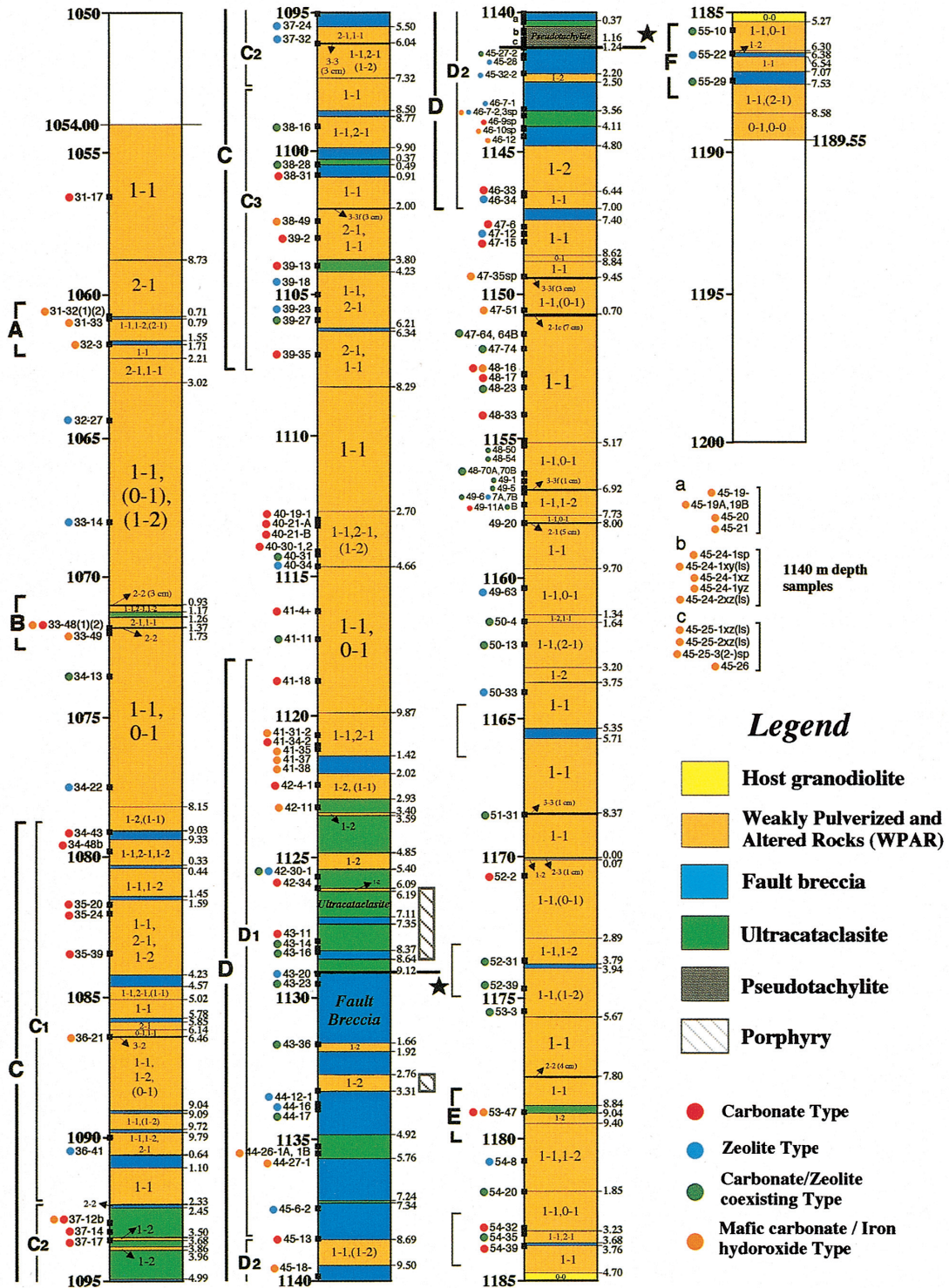


Fig. 5 Detailed fault rock distribution map for the depth range of from 1,054.00 to 1,189.55 m in the NIED core. The WPAR classification is indicated by numbers, e.g. 1-1 represents PI-AI, which is based on the criteria shown in Table 1. More than two classifications in a range indicate that the first one is predominant, and classifications noted in parentheses indicate the rare presence of that kind of WPAR. The depths are indicated at both right and left sides of the columns. The left ones show depths at 5 m intervals and the right ones show depths up to 1 cm order with an accuracy of ± 5 cm. The six major shear zones are indicated in gray parentheses with bold letters, and minor ones are just shown using gray parentheses. Samples and their depth ranges for microstructural examinations are indicated by small black rectangles with sample numbers. See text for further explanations.

fault zone, several shear zones, showing similar characteristics, are present.

Analysis of fault rock distribution clarifies the fact that the Nojima fault zone contains six major shear zones, from shallower to deeper levels, these are the A to F zones. Each shear zone is surrounded by the WPAR. Among these, the C and D zones are the candidates for the core zone of the Nojima fault for the following reasons. (1) The C and D zones are relatively thick as a whole, and have sub-shear zones (C1 to C3 and D1 to D2). (2) The C and D zones contain fault breccia, relatively thick ultracataclasite, and the D zone has a pseudotachylite layer. (3) Density, porosity, elastic wave velocity and other physical logging data show a distinct change or anomalies especially in these zones. The degree of change in these data is greater in the D zone than in the C zone (Ikeda *et al.*, 2001; Omura *et al.*, 2001), indicating that the D zone is more likely to have been activated during the 1995 earthquake. These results suggest that the C and D zones contain localized fault surfaces formed by co-seismic events and that the D zone might have been formed at more recent, including current, seismic events, while the C zone is consolidated, and thus is the older shear zone. Therefore, we offer a tentative definition of the Nojima fault surface as the fault surface that appeared at the bottom of the D2 subzone, the boundary between the ultracataclasite and fault breccia (1,141.24m depth). Results of mineral assemblage analysis (Matsuda *et al.*, 2001) indicate that the fault surface is a boundary between laumontite (hanging wall) and laumontite + stillbite (footwall) assemblages. This indicates that the fault surface at this depth has experienced large displacements with reverse components, since higher temperature assemblage appears at the shallower depths. Meanwhile, chemical composition data (Matsuda *et al.*, 2001) shows anomalously high concentrations of HFSE (High Field Strength Elements) around the depth of 1,125m, which corresponds to the D1 subzone. Concentration of HFSE is considered to be one of the typical characteristics of the frictional fault zone (Goddard and Evans, 1995; Evans and Chester, 1995). Thus, another candidate of the main fault surface of the 1995 event is at the boundary between the ultracataclasite and fault breccia in the center of the D1 subzone (1,129.12m depth, Fig. 5). In addition, it should also be noted that the A or B shear zone might have been activated during the 1995 earthquake, based on the distinct anomalies of geophysical logging data (Omura *et al.*, 2001).

The history of the evolution of the Nojima fault

zone in the NIED core, clarified by meso-and microscopic observations is as follows. Deformation and alteration of the WPAR overprint porphyry, suggests that the WPAR was formed after intrusion of porphyry. The WPAR is overprinted by fault breccia, which is further overprinted by ultracataclasite indicating the formation sequence of these fault rocks. A crosscutting relationship between micro shear surfaces and foliations both in the ultracataclasite and pseudotachylite shows that the pseudotachylite was formed after the ultracataclasite. The presence of an injection structure of the pseudotachylite into the ultracataclasite also supports this observation. From the above mentioned observations and considerations, it is possible to assert that fault rocks in the NIED 1,140m fault zone were basically formed in the following order (1) Host rocks, (2) Porphyry intrusive rock, (3) WPAR, (4) Fault breccia, (5) Ultracataclasite and (6) Pseudotachylite. This result suggests that every shear zone, including zones A to F were evolved from WPAR overprinting host rocks. Although there are several ultracataclasite zones present in the C and D zones, a lack of clear evidence of overprinting relationships among them precludes further interpretation of their formation sequence. However, it should be pointed out that the juxtaposition of several ultracataclasite layers and the absence of a clay gouge layer is one of the prominent features in the 1,140m fault zone of the NIED core, which contrasts with the characteristics observed at the GSJ Hirabayashi core (Tanaka *et al.*, 2000; Fujimoto *et al.*, in press; Ohtani *et al.*, 2000).

Three additional thin shear zones containing fault breccia are also recognized in the Nojima fault zone (Fig. 5). Although they may be regarded as nucleations of shear localization, further examinations are necessary to clarify this issue.

5.2 Characterization of each shear zone and the WPAR in the Nojima fault zone

Each shear zone shown in Fig. 5 is basically discriminated by the mode of fault rock distribution and by the deformation/alteration modes of fault rocks. Generally, each shear zone is centralized by the fault rocks that have experienced the heaviest pulverization and alteration, such as ultracataclasite, fault breccia, and pseudotachylite with MC/IH type alteration. Fault rocks in the hanging wall are characterized by C and C/Z type alteration, while those in the footwall are by Z type alteration. These contracting characteristics help distinguish between individual shear zones (Fig. 5). This trend is also common in the GSJ core (Tanaka *et al.*, 2000). Among the six major

shear zones distinguished in the NIED core, the A, B, E and F zones are less well characterized mainly due to the narrowness of these zones and the absence of microstructural data. Thus, we have omitted these zones from the present discussion in order to concentrate on clarifying the mechanisms of faulting during seismic cycles at shallow depths.

The C₂ subzone in the C zone and both subzones in the D zone (D₁ and D₂) have thick ultracataclasite layers. We will focus on the deformation and alteration of these three subzones. Microstructural observation of the fault rocks in the center zones of each subzone reveals that (1) the most dominant texture is random fabric and foliations are rarely observed, except in thin layers filled with MC/IH minerals developed in fault breccia and ultracataclasite, and (2) the wavy/spiral foliation, which is similar to the flow lines of turbulence are observed within dark brown clasts in the pseudotachylite layer in the D₂ zone (Fig. 4g, h). The former suggests that minor flow deformation likely occurred after the inflow of Fe³⁺ rich fluids into the core (part) of the shear zone. The latter suggests that fluidization or melting occurred during high velocity, co-seismic movement within the D² zone as proposed by Ohtsuki (2000). In the GSJ core, dark brown materials contained in the pseudotachylite are inferred to be graphite by chemical analysis (Tanaka *et al.*, 2000). If this is the case, the only possible origin of the graphite is the carbonate minerals or CO₂ gas, suggesting that deoxidation occurred in this pseudotachylite, possibly caused by frictional heating under the low oxygen conditions that are present during the co-seismic period (Tanaka *et al.*, 2000). From these considerations, it can be assumed that the D₂ shear zone was formed by localized, high-velocity frictional motion of the fault.

C type alteration, commonly observed at the hanging wall of each shear zone could be the result of surface water, since it generally contains a large amount of CO₂ gas. Dilatancy is a necessary characteristic for the inflow of such fluids into the zone. Thus, this zone could have been formed during co-seismic periods. The characteristics of Z type alteration at the footwall of each shear zones are as follows; (1) abundant zeolite veins in the matrix of hydraulically brecciated rock, and (2) feldspar crystals being mainly altered to zeolite. Co-seismic activity of this zone is clearly evidenced by (1), which also suggests the super-hydrostatic condition of the footwall of each shear zone at the seismic faulting. The fact of (2) also implies a slower rate of fluid flow containing similar chemical composition of plagioclase. From

these considerations, the footwall of each shear zone could have been a fluid-rich, co-seismic brecciation zone during seismic cycles. This fluid could be derived from a slower flow rate through the intracrystalline path in feldspars, which is then trapped in this shear zone. The fluid is possibly of deeper origin, because the relatively thick, impermeable layers of the fine grained material in the fault core (ultracataclasite and pseudotachylite) (Naka *et al.*, 1998; Lockner *et al.*, 2000) preclude the down flow of fluids of meteoric origin.

The WPAR is widely distributed, surrounding the every shear zone in the NIED core. During post- and interseismic periods they could be the conduit for fluid flow, due to the opening of cracks and dilatancy caused by seismic failure (Caine *et al.*, 1996; Seront *et al.*, 1998; Caine and Forster, 1999). This could be proved by the presence of euhedral, large grains of carbonate and zeolite filling cracks.

5.3 Mechanical roles of each shear zone during seismic cycle in the Nojima fault

Recently the concept of a shear zone architecture has undergone major revisions mainly based on microstructural observations, chemical measurements and permeability measurements (Chester and Logan, 1986; Chester *et al.*, 1993; Evans and Chester, 1995; Goddard and Evans, 1995; Caine *et al.*, 1996; Caine and Forster, 1999; Evans *et al.*, 1997; Lockner *et al.*, 2000). To date, two distinct zones have been recognized in the fault zone from these results. One is the fault core, which is characterized by relatively low shear strength and very low permeability mainly caused by very-fine grained nature of the fault rocks in this zone. Another is the damaged zone, which has a tabular form and surrounds the fault core. The damaged zone is characterized by moderate strength and moderate to high permeability (Lockner *et al.*, 2000). These two zones are further surrounded by the protolith (host rock) which shows a higher shear strength and very low permeability. The fault core-damaged zone model is quite reasonable as a means of understanding the fault zone architecture and the mechanics of the Nojima fault zone in the NIED core at a depth of 1,140m. We will attempt to construct a realistic model because we now have a detailed understanding of the fault rock distribution as a result of a vast amount of core observation of polished surfaces and microstructural observations of 134 thin sections, as described so far. Figure 6 shows a mechanism map of the fault zone of the NIED core at a depth of around 1,140m. Physical logging results, mesoscopic and microstructural observations all indicate that the

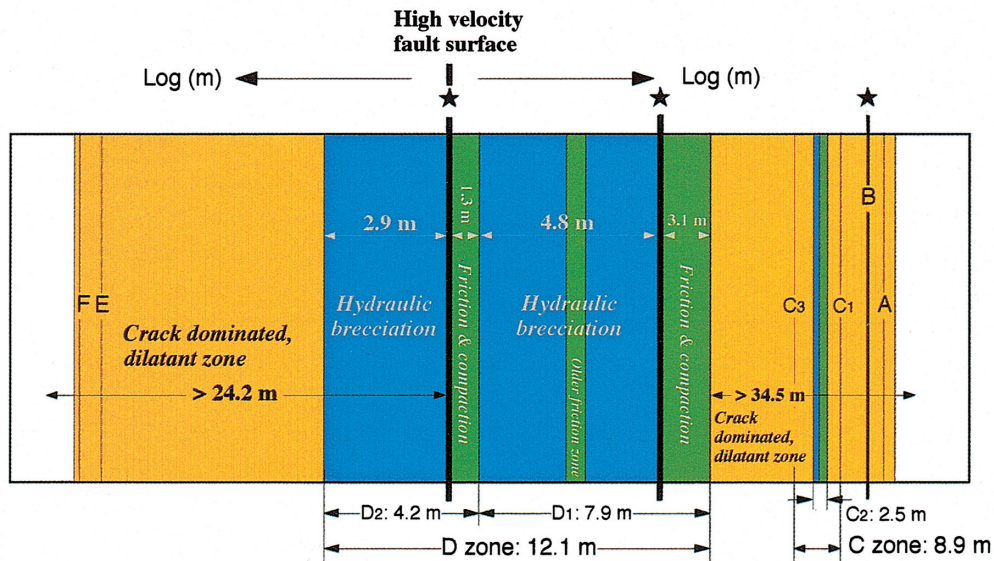


Fig. 6 Mechanism map of the Nojima fault zone interpreted from fault rock distribution and meso-/microstructural observation, showing that several, high velocity shear zones exist in a fault zone. The thickness of the fault zone is presented using the log scale. See text for detailed explanations.

centralized zone in the Nojima fault zone is the D₂ and/or D₁ shear zone. Both zones are composed of three parts, each of which played a different role during earthquakes. The hanging wall of the shear zone is characterized by dilatant, crack dominated deformation and inflow of CO₂ rich fluids which are possibly of surface water origin. This part may play the role of the trapped zone for surface fluid during an interseismic period and the hydraulic brecciation zone during a coseismic period. Microtextural characteristics of the footwall of the shear zone are basically similar to the hanging wall. However, Z type alterations are prominent instead of C type alterations. Where minor C type alteration is observed, it overprints the Z type alteration. Thus, the footwall shear zone may be formed by one of the following two mechanisms. (1) Z type alteration occurring throughout the fault zone at older stages, and somehow being preserved in the footwall shear zone. (2) Z type alteration occurring during recent interseismic periods especially at the footwall which have played the role of hydraulic brecciation zone during coseismic periods. Although, both cases are possible, it should be pointed out that fluid flow in the hanging wall has not connected with that in the footwall shear zone, since the mode of alteration differs between the two.

The centralized layer of the shear zone is characterized by the highly fine grained nature of the fault rocks, the absence of veins filled with secondary

minerals, and possible evidence of heat generation and minor flow deformation where iron hydroxide minerals are precipitated. These features suggest that the centralized layers of the shear zones could play the role of frictional, high-velocity, large displacement zone during coseismic periods. Precipitation of iron hydroxide minerals and minor flow deformation within them may represent an inflow of Fe³⁺ rich fluid during a coseismic period and post seismic creep deformation. A common characteristic of the center zone of the fault is a very fine grained nature of the matrix of fault rocks, suggesting that the core could be a fluid barrier during interseismic periods (Chester *et al.*, 1993 ; Lockner *et al.*, 2000). This consideration would be supported by the fact that alteration mode is different between the hanging and footwalls.

Few clay-rich shear zones were observed in the NIED core at the depth of 1,140m, which was observed in the GSJ core and which is regarded as an interseismic, creeping shear zone by Tanaka *et al.* (2000). Instead, many thin layers (<1 cm thick) showing "flow texture" filled with clay, iron hydroxide and self crushing materials are distributed throughout the fault, suggesting that the creep zone may not be localized at this depth. Dominant flow textures are observed at the 1,300m fault zone (Kobayashi *et al.*, 2001), suggesting another possible explanation, that the 1,300 m fault zone could have a function of flow deformation.

6. Conclusion

We have performed fault rock distribution analysis and microstructural observations on deformation and alteration throughout the shear zone at a depth of 1,140m in the NIED core. These data lead to the following conclusions.

The whole fault zone is thicker than 67m in and contains six major shear zones which are denoted as shear zones A to F becoming gradually deeper. Every shear zone is surrounded by weakly pulverized and altered fault-related rocks (WPAR). Detailed microstructural observations have been performed for the C and D shear zones. Both shear zones have subzones (C_1 to C_3 , and D_1 and D_2), which have formed during recent activities of the Nojima fault. However, the C zone was formed at an early, older stage than the D zone.

The C and D zones are located at depths of around 1,095m and 1,140m, respectively. Both zones are characterized by random fabric fault breccia, ultracataclasite and pseudotachylite. The microstructural examination clarifies that these zones are regarded as the high-velocity co-seismic zones associated with heat generation. The hanging wall and the footwall of these two zones are characterized by dominant hydraulic brecciation texture. These zones are regarded as a fluid trapped zone formed during the post-/interseismic periods and a hydraulic explosion zone formed during the coseismic periods. The fact that the mode of alteration in the hanging wall (C type) is different from that in the footwall (Z type) suggests that center zones of the fault (C, D zones) would have acted as the fluid barrier during interseismic periods. Broadly, the C and D shear zones are regarded as the co-seismic fault core, in which each part behaves differently. There is no clay rich, slow velocity creeping zone in this depth range of the NIED core. This may suggest that the creep zone is located at another depth range, or that creeping may have occurred in scattered thin shear zones. The WPAR surrounding these shear zones is characterized by numerous cracks containing carbonate and zeolite minerals. This zone is regarded as a dilatant, co-seismic zone at the marginal part of the main shear surfaces, and as a fluid conduit during post- / interseismic periods.

Acknowledgements

We would like to thank to A. Yamasaki, T. Sawaguchi of Waseda University and N. Tomida of Ehime University for their effort to help preparing huge number of core slabs.

References

- 1) Awata, Y., Mizuno, K., Sugiyama, Y., Imura, R., Shimokawa, K., Okumura, K., and Tsukuda, E. (1996) : Surface fault ruptures on the Northwest coast of Awaji Island associated with the Hyogo-ken Nanbu earthquake of 1995, Japan (in Japanese with English abstract). *J. Seis. Soc. Japan*, **49**, 113-124.
- 2) Caine, J.S., Evans, J.P., and Forster, C.B. (1996) : Fault zone architecture and permeability structure. *Geology*, **24**, 1025-1028.
- 3) Caine, J.S. and Forster, C.B. (1999) : Fault zone architecture and fluid flow : insights from field data and numerical modeling. in *Faults and Subsurface Flow in the Shallow Crust*, AGU Geophysical Monograph Series, **113**, edited by W. Haneberg, P. Mozley, J. Moore, and L. Goodwin, Amer. Geophys. Union., Washington, D.C..
- 4) Chester, F.M. and Logan, J.M. (1986) : Implications for mechanical properties of brittle faults from observations of the Punchbowl fault zone, California. *Pure and Applied Geophysics*, **124**, 79-106.
- 5) Chester, F.M., Evans, J.P. and Biegel, R.L. (1993) : Internal Structure and weakening mechanisms of the San Andreas Fault. *J. Geophys. Res.*, **98**, 771-786.
- 6) Evans, J.P. and Chester, F.M. (1995) : Fluid-rock interaction in faults of the San Andreas system : Inferences from San Gabriel fault rock geochemistry and microstructures. *J. Geophys. Res.*, **100**, 13007-13020.
- 7) Evans, J.P., Forster, C.B. and Goddard, J.V. (1997) : Permeability of fault-related rocks, and implications for hydraulic structure of fault zones. *J. Struct. Geol.*, **19**, 1391-1402.
- 8) Fujimoto, K., Tanaka, H., Higuchi, T., Tomida, N., Ohtani, T., and Ito, H. Alteration and mass transfer along the NIED Hirabayashi borehole penetrating the Nojima fault, Japan. *The Island Arc*, in press.
- 9) Goddard, J.V. and Evans, J.P. (1995) : Chemical changes and fluid-rock interactions in faults of crystalline thrust sheets, northwestern Wyoming, U.S.A.. *J. Struct. Geol.*, **17**, 553-547.
- 10) Higgins, M.W. (1971) : Cataclastic rocks. *Prof. Pap. U. S. Geol. Surv.*, 687pp.
- 11) Ikeda, R., Omura, K., Iio, Y., Arai, T., Kobayashi, K., Shimada, K., Tanaka, H., Tomita, T., Hirano, S., and Matsuda, T. (2001) : Drilling investigation through the Nojima fault of the 1995 Hyogo-ken Nanbu earthquake, Japan (in Japanese with English abstract). Report of the National Research Institute for Earth Science and Disaster Prevention, No. **61**, 141-153.
- 12) Kobayashi, K., Arai, T., Ikeda, R., Omura, K., Shimada, K., Tanaka, H., Tomita, T., Hirano, S., and Matsuda, T. (2001) : Textures of fault rocks in the

- fracture zone of the Nojima fault at a depth of 1,300 m : observations from Hirabayashi NIED drilling core (in Japanese with English abstract). Report of the National Research Institute for Earth Science and Disaster Prevention, No. **61**, 223-229.
- 13) Lin, A. and Uda, S. (1996) : Morphological characteristics of the earthquake surface rupture which occurred on Awaji Island, associated with the 1995 Southern Hyogo Prefecture Earthquake. *The Island Arc*, **5**, 1 -15.
- 14) Lockner, D.A., Naka, H., Tanaka, H., Ito, H., and Ikeda, R. (2000) : Permeability and strength of core samples from the Nojima Fault of the 1995 Kobe Earthquake. in Proceedings of the International Workshop on the Nojima Fault Core and Borehole Data Analysis, GSJ Interim Report No. EQ/00/1 and USGS Open file Report 00-129, edited by H. Ito, K. Fujimoto, H. Tanaka, and D.A. Lockner, 147-152.
- 15) Matsuda, T., Arai, T., Ikeda, R., Omura, K., Kobayashi, K., Shimada, K., Tanaka, H., Tomita, T., and Hirano, S. (2001) : Chemical analysis along fracture zones (1,140m, 1,300m, 1,800m depth) of the Hirabayashi NIED drilling core of the Nojima fault (in Japanese with English abstract). Report of the National Research Institute for Earth Science and Disaster Prevention, No. **61**, 183-193.
- 16) Mizuno, K., Hattori, H., Sangawa, A., and Takahashi, Y. (1990) : Geology of the Akaishi District (in Japanese with English abstract), With Geological Sheet Map at 1 : 50,000. Geological Survey of Japan, 90pp.
- 17) Naka, H., Lockner, D.A., Tanaka, H., Ikeda, R., and Ito, H. (1998) : Strength and permeability of core samples taken from drillholes crossing the Nojima fault (abstract). *EOS Trans. AGU*, **78**, p823.
- 18) Nakata, T., Yomogida, K., Okada, J., Sakamoto, T., Asahi, K., and Chida, N. (1995) : Surface fault ruptures associated with the 1995 Hyogo-ken Nanbu earthquake (in Japanese with English abstract). *J. Geograph.*, **104**, 127-142.
- 19) Ohtani, T., Fujimoto, K., Ito, H., Tanaka, H., Tomida, N., and Higuchi, T. (2000) : Fault rocks and past to recent fluid characteristics from the borehole survey of the Nojima fault ruptured in the 1995 Kobe earthquake, southwest Japan. *J. Geophys. Res.*, **105**, 16161 -16171.
- 20) Ohtsuki, K. (2000) : Thermal pressurization, fluidization and melting of fault gouge during seismic slip recorded in the rock from Nojima Fault. in Proceedings of the International Workshop on the Nojima Fault Core and Borehole Data Analysis, GSJ Interim Report No. EQ/00/1 and USGS Open file Report 00 -129, edited by H. Ito, K. Fujimoto, H. Tanaka, and D.A. Lockner, 43-50.
- 21) Omura, K., Ikeda, R., Iio, Y., Arai, T., Kobayashi, K., Shimada, K., Tanaka, H., Tomita, T., Hirano, S., and Matsuda, T. (2001) : Characteristics of logging data for fracture zones in Hirabayashi NIED borehole drilling through Nojima fault (in Japanese with English abstract). Report of the National Research Institute for Earth Science and Disaster Prevention, No. **61**, 155-171.
- 22) Seront, B., Wong, T.F., Caine, J.S., Forster, C.B., and Bruhn, R.L. (1998) : Laboratory characterization of hydromechanical properties of a seismogenic normal fault system. *J. Struct. Geol.*, **20**, 865-881.
- 23) Sibson, R.H. (1977) : Fault rocks and fault mechanisms. *J. Geol. Soc. Lond.*, **133**, 191-213.
- 24) Takahashi, Y. (1992) : K-Ar ages of the granitic rocks in Awaji Island-with an emphasis on timing of mylonitization-(in Japanese with English abstract). *J. Min. Petrol. Economic Geol.*, **87**, 291-299.
- 25) Tanaka, H. and Itaya, T. (1998) : Fault zone rocks deep beneath the active fault. From the view point of structural petrology (in Japanese with English abstract). *Kagaku*, **68**, 246-254.
- 26) Tanaka, H., Higuchi, T., Tomida, N., Fujimoto, K., Ohtani, T., and Ito, H. (1999) : Distribution, deformation and alteration of fault rocks along the GSJ core penetrating the Nojima Fault, Awaji Island, Southwest Japan (in Japanese with English abstract). *J. Geol. Soc. Japan*, **105**, 72-85.
- 27) Tanaka, H., Tomida, N., Sekiya, N., Tsukiyama, Y., Fujimoto, K., Ohtani, T., and Ito, H. (2000) : Distribution, deformation and alteration of fault rocks along the GSJ core penetrating the Nojima fault, Awaji Island, Southwest Japan. in Proceedings of the International Workshop on the Nojima Fault Core and Borehole Data Analysis, GSJ Interim Report No. EQ/00/1 and USGS Open file Report 00-129, edited by H. Ito, K. Fujimoto, H. Tanaka, and D.A. Lockner, 81-101.
- 28) The Research Group for Active Faults of Japan (1991) : Active Faults in Japan (in Japanese with English abstract) : Sheet Maps and Inventories (Revised Edition). University of Tokyo Press, Tokyo, 437pp.
- 29) Zoback, M.D. and Lachenbruch, A.H. (1992) : Introduction to special section on the Cajon Pass scientific drilling project. *J. Geophys. Res.*, **97**, 4990-4994.
- 30) Zoback, M.D. Silver, L.T., Henyey, T., and Thatcher, W. (1988) : The Cajon Pass scientific drilling experiment ; Overview of Phase I. *Geophys. Res. Lett.*, **15**, 933-936.

(Accepted : December 4, 2000)

Appendix Results of microtextural observations of fault rocks under the optical microscope.

Appendix Results of microtextural observations of fault rocks under the optical microscope.

Appendix Results of microtextural observations of fault rocks under the optical microscope.

Appendix Results of microtextural observations of fault rocks under the optical microscope.

A	1105.567	39-23	2:1; WPAR (Z)	-	Host framework texture, tracks, mbs (fine-grained carbonate + self-crushed fragments)	Trans (circular zoeline), trans (small amounts of thin carbonate vein)	Ribbon carbonate	Common	Hydration and softening in some grains	Decrease	Small numbers of pseudomorphs	Lost		
A	1105.558	39-27	1:1; WPAR (C/Z)	-	Host framework texture, tracks, mbs (fine-grained carbonate + self-crushed fragments)	Trans (carbonate), trans (zoeline)	Sericite, small amounts of carbonate.	-	-	-	WPAR between C1 shear zone. Zeolite type WPAR.	Lower part of C1 shear zone. Zeolite type WPAR.		
A	1107.162	39-35	2:1; WPAR (C)	Moderate (mbsz)	Host framework texture, tracks, mbs (self-crushed fragments, zoeline, carbonate)	Trans (carbonate), trans (zoeline)	Weak fragmentation by thin veins of carbonate, intercalated within zeolite matrix (hydraulic brecciation)	Sericite, small amounts of carbonate.	Ribbon carbonate, ribbon zoeline	Predominant	Hydration and softening in some grains	Decrease	Small numbers of pseudomorphs	Lost
C	1112.556	40-19-1	2:1; WPAR (C)	Moderate (mbsz)	Host framework texture, tracks, mbs (self-crushed fragments, zoeline, carbonate)	Trans (carbonate); intra (small amounts of zoeline)	Weak fragmentation by thin veins of carbonate, intercalated within zeolite matrix (hydraulic brecciation)	Sericite, small amounts of carbonate.	Spherule carbonate	Predominant	Hydration and softening in some grains	Decrease	1 grain of deformed pseudomorph	WPAR between C/D shear zone. Carbonate type.
C	1113.101	40-21A	1:1; WPAR (C) part	Moderate (mbsz)	Random fabric: matrix (dark brown carbonate), self-crushed fragments (self-crushed, cracks, intra + self-crushed fragments + dark brown carbonate)	Trans (carbonate); intra (small amounts of zoeline)	Quartz-W-EX + B-EX, feldspar weak W-EX	Predominant	Spherule carbonate	Predominant	N/A because of few residual grains	Almost lost (1 grain remains)	1 grain of deformed pseudomorph	WPAR between C/D shear zone. Carbonate type.
C	1113.209	40-21B	1:1; Carbonate type WPAR (mbst)	High (mbsz)	Random fabric: matrix (fine-grained carbonate), self-crushed fragments (self-crushed, cracks, intra + self-crushed fragments, intra + self-crushed fragments)	Trans (matrix carbonate)	Replaced by dark brown carbonate spot. Replacement by zoeline + sercite	Spherule carbonate	Predominant	Hydration and softening in some grains	Extremely decrease	1 grain of deformed pseudomorph	WPAR between C/D shear zone. Carbonate type.	
C	1114.101	40-39-1	2:1; WPAR (C)	-	Host framework texture, tracks, mbs (fine-grained carbonate + self-crushed fragments, intra + self-crushed fragments)	Trans (carbonate), trans (zoeline)	Quartz-W-EX + B-EX, feldspar weak W-EX besides mbsz	Predominant, hydraulic brecciation texture in quartz	Spherule carbonate	Predominant	Common hydration staining	Extremely decrease	No pseudomorphs	WPAR between C/D shear zone. Zeolite type.
C	1114.101	40-39-2	2:1; WPAR (Z)	Moderate (mbsz)	Perpendicular framework texture, tracks, mbs (fine-grained carbonate + self-crushed fragments, intra + self-crushed fragments)	Trans (carbonate), trans (zoeline)	Predominant in mbsz. Hydraulic brecciation texture in quartz	Spherule carbonate, ribbon zoeline vein in some grains	Predominant	Common hydration staining	Extremely decrease	1 grain of deformed pseudomorph	WPAR between C/D shear zone. Zeolite type.	
C	1114.217	40-31	1:1; WPAR (C/Z)	Moderate (mbsz)	Host framework texture, tracks, mbs (fine-grained dark brown material + clastic fragments, intra + self-crushed fragments)	Trans (carbonate), trans (zoeline)	Quartz-W-EX + B-EX, feldspar weak W-EX	Predominant in mbsz. Hydraulic brecciation texture in quartz	Spherule carbonate, ribbon zoeline vein in some grains	Predominant	Hydration and softening in some grains	Extremely decrease	Pseudomorphs	WPAR between C/D shear zone. Zeolite type.
C	1114.664	40-34	3:1; Ultrareactivedolomite (Z)	-	Random fabric: matrix (fine-grained carbonate), self-crushed fragments (self-crushed, cracks, intra + self-crushed fragments, intra + self-crushed fragments)	Trans (matrix carbonate)	Only quartz grains are remaining, rock broken	Predominant	Predominant	Extremely decrease	No pseudomorphs	Lost	No pseudomorphs	U/calc zone between C/D shear zone. Zeolite type (minor).

Appendix Results of microtextural observations of fault rocks under the optical microscope.

C	1116.273	41-44	1:1; WPAR (C)	-	Host framework texture, cracks, fine-grained carbonate + fine-grained sand (remained fragments)	Trans (siltstone), trans (carbonate);	Hydraulic brecciation	Spherule carbonite, rhombic zelite vein	Hydration softening in some grains.	Replaced carbonate	Extremely decrease	Small numbers of deformed pseudomorphs	Lost	
C	1117.268	41-41	0:1; WPAR (C/Z)	-	Host framework texture, cracks, fine-grained zelite + fine-grained sand (remained fragments)	Trans (siltstone), trans (carbonate);	Hydraulic brecciation	Spherule carbonite, zelite, selenite, scericite	Hydration softening in some grains.	Replaced carbonate	Extremely decrease	Small numbers of deformed pseudomorphs	Lost	
C	1118.731	41-18	1:1; WPAR (C)	-	Host framework texture, Cracks, 1. mbsz (clay + silt-crushed fragments + carbonate), 2. mbsz (clay + silt-crushed fragments + carbonate), 3. mbsz (clay + silt-crushed fragments)	Trans (carbonate)	Hydraulic brecciation	Spherule carbonite, rhombic zelite	Hydration softening in some grains.	Replaced carbonate	Extremely decrease	Pseudomorphs	Lost	
C	1120.668	41-31-2	2-1c; WPAR (MC)	-	Host framework texture is barely preserved. Cracks, mbsz (dark brown fine-grained carbonate) + fine-grained sand (remained fragments) + fine-grained clay + silt-crushed fragments + carbonate, some grains) mbsz (zelite + selenite + fragments + small amounts of dark brown carbonate).	Trans (zelite) + trans (carbonate) (thin vein.)	Predominant carbonate spots	Predominant carbonate	Hydration softening in some grains.	Replaced carbonate	Extremely decrease	Pseudomorphs	Lost	
C	1121.013	41-34-2	1:1; WPAR (C) (in mbsz)	Moderate	Random fabric: matrix (fine-grained dark brown/matic carbonite + fine-grained silt-carbonate) mbsz (dark brown/matic fragments) + clay + clast (self-crushed fragments) + matic carbonate)	Trans (matrix carbonate)	Quartz, weak W-EX + B-EX, elongate weak W-EX	Predominant	Hydration softening in some grains.	Replaced carbonate	Extremely decrease	Pseudomorphs	Lost	
C	1121.192	41-35	1:1; WPAR (MC) (in fine grained Xerolith)	High	Host framework texture. Cracks, mbsz (dark brown (fine-grained material (seismic slip surface?)) + self-crushed fragments), mbsz (brown (fragments) + clay) + clast (carbonate) material + silt-carbonate fragments + matic carbonate) + some laminae of clay)	Trans (matrix carbonate)	Quartz, weak W-EX	Less prominent	Carbone spots, sericitic, iron hydroxide spots in one grain	Spherule carbonite	-	-	No pseudomorphs	Lost
C	1121.422	41-37	2-1; WPAR (MC) (in breccia)	Moderate	Random fabric: matrix (fine-grained sand + silt-crushed fragments + clay) + clast (self-crushed fragments + matic carbonite, mbsz (brown (fragments) + clay) + clast (self-crushed fragments + matic carbonate) + some laminae of clay in center zones)	No vein	Quant. W-EX + W-EX, elongate class: W-EX	Predominant, especially in ultraclastic zone.	Spot of fine grained carbonate	Hydration softening	A few residual grains of carbonate	Almost lost	No pseudomorphs	Lost
C	1121.577	41-38	2-2; Fault breccia (foliated) (MC)	Moderate	Random fabric: matrix (fine-grained sand-crushed fragments + clay) + clast (self-crushed fragments + matic carbonate, mbsz (brown (fragments) + clay) + clast (self-crushed fragments + matic carbonate) + some laminae of clay in center zones)	No vein	Quant. W-EX + B-EX, elongate class: W-EX	Predominant, especially in ultraclastic zone.	Spot of fine grained carbonate	Hydration softening	A few residual grains of carbonate	Almost lost	No pseudomorphs	Lost
C	1122.426	42-41	1-2; WPAR (C)	Moderate	Host framework texture, fine-grained sand-crushed fragments + clay + clast (self-crushed fragments + matic carbonate, mbsz (brown (fragments) + clay) + clast (self-crushed fragments + matic carbonate) + some laminae of clay in center zones)	Trans (carbonate)	Quartz, W-EX + B-EX, elongate, mbsz	Predominant	Change color into grayish white (chalcocite?)	Replaced carbonate	Extremely decrease	Small numbers of pseudomorphs	Lost	
C	1123.201	42-11	2-2; Ultraclasticite (MC)	Moderate	Random fabric: matrix (fine-grained sand-crushed fragments + clay) + clast (self-crushed fragments + matic carbonate, mbsz (brown (fragments) + clay) + clast (self-crushed fragments + matic carbonate) + some laminae of clay in center zones)	Trans (carbonate)	Quartz, W-EX, elongate, mbsz	Dominant	Spot of fine grained carbonates	Hydration softening	Extremely and involved into matrix	Almost lost	No pseudomorphs	Lost
C	1125.606	42-30-1	2-3; Ultraclasticite (C/Z)	Moderate	Random fabric: matrix fine-grained sand-crushed fragments + large amount of fine-grained zelite + clast (self-crushed fragments, fragments of zelite vein, cracks)	Trans (carbonate), predominant	Quartz, W-EX + B-EX, elongate	Zelite replacement (in some parts of fine grained carbonates)	Change color into grayish white (chalcocite?)	Replaced carbonate	Extremely and involved into matrix	Almost lost	No pseudomorphs	Lost

Appendix Results of microtextural observations of fault rocks under the optical microscope.

C	1126.990	42-24.5	2-3: Fault breccia hydraulic brecciation	Moderate	Random fabric, matrix (carbonate + clst self-crushed fragments), cracks, imbricate (self-crushed fragments + carbonate) material, (US fabric present)	Trans (carbonate), trans (zeolite)	Quartz-W.EX. + B.EX., feldspar-W.EX.	Hydraulic brecciation	Spherule matrix carbonate	Predominant	Hydration softening	Extremely decrease	Deformed pseudomorphs	Lost	Moderate part of D1 shear zone. Carbonate type. Fault brecciation with hydraulic brecciation texture.
C	1127.972	43-11	1-2: Altered intrusive rock (CZ)	High	Host framework texture, cracks, fissile self-crushed fragments, cracks, imbricate (self-crushed fragments + carbonate) material, (US fabric present)	Trans (carbonate), trans (zeolite)	N/A because of very fine grain size	Spots of fine grained carbonates	Spherule matrix carbonate (brown interference color)	Predominant	-	-	-	-	Middle part of D1 shear zone. Sheared and altered intrusive rocks (coexisting type).
A	1128.232	43-14	2-2: Fault breccia (CZ) altered and brecciated intrusive rock	-	Host framework texture + s-clst (self-crushed fragments + carbonate) matrix, (US fabric present)	Trans (carbonate), which cut the mass, with moderate dips, trans (zeolite)	Quartz, fine grain size due to intrusive body origin, W.EX. (7), feldspar, weak W., EX	N/A because of very fine grain size	Spots of fine grained carbonates, small amounts of sericitic, zeolite replacement in some grains	Predominant	-	-	-	-	Lower part of D1 shear zone. Sheared and altered intrusive rocks (coexisting type).
A	1128.370	43-16	2-2: Fault breccia (CZ) altered and brecciated intrusive rock	High (vein)	Random fabric, matrix (self-crushed fragments + carbonate) matrix, (US fabric present)	Trans (carbonate), trans (zeolite)	Quartz, fine grain size due to intrusive body origin, W.EX. (7), feldspar, weak W., EX	N/A because of very fine grain size	Spots of fine grained carbonates, small amounts of sericitic, zeolite replacement in some grains	Predominant	-	-	-	-	Lower part of D1 shear zone. Sheared and altered intrusive rocks (coexisting type).
A	1129.121	43-20	2-3: Fault breccia (Z)	Low	Random fabric, matrix (self-crushed fragments + carbonate) matrix, (US fabric present)	Trans (carbonate), trans (zeolite)	Quartz-W.EX., feldspar-equan	Predominant	Spherule matrix carbonate (brown interference color)	Predominant	-	-	-	-	Lower part of D1 shear zone. Zeolite type. Fault breccia, containing carbonatic veins.
A	1129.498	43-23	2-2: Fault breccia (Z) (C overprints)	Moderate	Random fabric, matrix (self-crushed fragments + carbonate) matrix, (US fabric present)	Trans (carbonate), trans (zeolite)	Quartz-W.EX. + weak B.EX., feldspar, weak W., EX	Predominant, especially in mbs	Spherule matrix carbonate	Predominant	-	-	-	-	Lower part of D1 shear zone. Zeolite type. Fault breccia, containing carbonatic veins.
C	1131.662	43-36	1-2: WPAR (C/Z)	Moderate	Fissile framework texture, cracks, fissile self-crushed fragments, small amounts of clay	Trans (carbonate), trans (zeolite)	Quartz-W.EX. + weak B.EX.	Common	Spherule matrix, some zeolite spots in some grains	Predominant	Small amount of softening bending	Extremely decrease	Small numbers of pseudomorphs	Lost	Lower part of D1 shear zone. Zeolite type. Fault breccia, containing carbonatic veins.
C	1133.306	44-12-1	1-2: WPAR originates from intrusive rock (CZ)	-	Host framework texture, cracks, imbricate (self-crushed fragments + carbonate) matrix, (US fabric present)	Trans (zeolite), trans (carbonate)	Quartz-N/A because of very fine grained nature of intrusive rocks, W., EX	N/A because of very fine grain size	Predominant, some zeolite in some grains	Predominant	-	-	-	-	Lower part of D1 shear zone. Weekly sheared, altered intrusive rocks.
C	1133.770	44-16	2-2: Fault breccia (Z)	-	Host framework texture, cracks, imbricate (self-crushed fragments + carbonate) matrix, (US fabric present)	Trans (carbonate), trans (zeolite)	Quartz-W.EX. + weak B.EX.	Common	Zeolite, spots of fine-grained carbonates	Predominant	Kink bands in two grains (softening and bending)	Almost lost	No pseudomorphs	Lost	Lower part of D1 shear zone. Coexisting type. Fault breccia
C	1133.936	44-17	3-3: Ultratacasite (CZ)	Moderate	Random fabric, matrix (self-crushed fragments + carbonate) matrix, (US fabric present)	Trans (carbonate)	Quartz, feldspar, feldspar, N/A due to few residual grains	Predominant	-	-	-	-	-	-	Lower part of D1 shear zone. Coexisting type. Ultratacasite.
C	1135.248	44-26-1A	3-3: Ultratacasite (MC)	High	Random fabric, matrix (fine-grained carbonate + self-crushed fragments + clst (self-crushed fragments + carbonate)) matrix, (US fabric present)	Trans (carbonate)	Quartz, feldspar, Weak-W.EX. (less treatments due to very fine grain size)	Predominant	N/A due to few residual grains	Predominant	-	-	-	-	Lower part of D1 shear zone. Matrix carbonatite type. Ultratacasite. Flow feature is prominent where the fine grained carbonates dominate.
C	1135.248	44-26-1B	3-3: Ultratacasite (MC)	High	Random fabric, matrix (fine-grained carbonate + self-crushed fragments + clst (self-crushed fragments + carbonate)) matrix, (US fabric present)	Trans (carbonate)	Quartz, feldspar, Weak-W.EX. (less treatments due to very fine grain size)	Predominant	N/A due to few residual grains	Predominant	-	-	-	-	Lower part of D1 shear zone. Matrix carbonatite type. Ultratacasite. Flow feature is prominent where the fine grained carbonates dominate.

Appendix Results of microtextural observations of fault rocks under the optical microscope.

Appendix Results of microtextural observations of fault rocks under the optical microscope.

Appendix Results of microtextural observations of fault rocks under the optical microscope.

Appendix Results of microtextural observations of fault rocks under the optical microscope.

C	1146,508	46-34	2-2: Fault breccia (2) overprinted by (C)	Random fabric: matrix (zoilite), self-crushed fragments + clast (self-crushed fragments), zoilite aggregates, cracks Host framework texture, cracks, mbsz (self-crushed fragments), trans (carbonate), overprinting residual grains due to shear.	Trans (carbonate)	Predominant	Replacement of zoilite is predominant	Spherical carbonate	Predominant	Hydration softening	-	Extreme decrease	-	Lost	
C	1147,617	47-6	1-1: WPAR (C)	-	-	Restriced within mbsz	Spots of fine grained carbonate	-	Hydration softening	-	Extreme decrease	No pseudomorphs	No	Lost	
C	1147,863	47-12	1-1: Zoilite type (less altered) WPAR (Z)	Host framework texture, cracks, mbsz (self-crushed fragments), trans (zoilite thin vein); trans (zoilite thin vein)	Quartz, weak W, EX, feldspar, weak W-EX	Restriced within mbsz	Zoilite predominant	Rare	Kink band	-	Decrease	Pseudomorphs	Lost	Just beneath the D shear zone. Carbonate type WPAR.	
C	1148,153	47-15	1-1: Carbonate type WPAR (C)	Host framework texture, cracks, mbsz (self-crushed fragments), biotite remains in the matrix, olivine, pyroxene, magnetite + clast (self-crushed rounded fragments + zoilite + carbonate aggregates)	Trans (carbonate), overprinting mbsz (self-crushed fragments), biotite	Restriced within mbsz	Spots of fine grained carbonate	Common	Hydration softening	-	Extreme decrease	No pseudomorphs	No	Just beneath the D shear zone. Upper part of fault mixed breccia zone. Carbonate type WPAR	
C	1149,398	47-35ep	1-3: Ultratacasite (MC)	N/C	-	-	-	-	-	-	-	No pseudomorphs	No	Beneath the D shear zone. Mafic carbonate type, minor ultratacasite zone	
C	1150,532	47-51	1-1: WPAR (MCH/H)	Horizontal	Quartz, weak W-EX, feldspar, weak W-EX	Restriced within mbsz	Spots of fine grained carbonate, predominantly	Rare	Kink band	Restricted with mbsz	Decrease	Pseudomorphs	Lost	Beneath the D shear zone. Mafic carbonate / non hydroyde type WPAR.	
C	1151,394	47-64	1-1: WPAR (CZ)	Moderate	Quartz, W-EX + W-EX	Restriced within mbsz	Zoilite, spots of fine grained carbonate	Predominant	Hydration softening	-	Decrease	No pseudomorphs	No	Beneath the D shear zone. Carbonate type overprint zoilite alteration	
C	1151,394	47-64B	1-1: WPAR (CZ)	Host framework texture, cracks, mbsz (self-crushed fragments), trans (carbonate), trans (zoilite)	Quartz, weak W-EX, feldspar, weak W-EX	Restriced within mbsz	Spots of fine grained carbonate	Predominant	Hydration softening	-	Decrease	Pseudomorphs	Lost	Beneath the D shear zone. Carbonate type overprint zoilite alteration	
C	1151,800	47-74	1-1: WPAR (CZ)	Low (mbsz)	Host framework texture, cracks, mbsz (self-crushed fragments), trans (carbonate), trans (zoilite), mafic carbonates	Quartz, weak W-EX, feldspar, weak W-EX	Restriced within mbsz	Zoilite, being overprinted by spots of fine grained carbonate	-	-	-	No pseudomorphs	No	Beneath the D shear zone. Carbonate type overprint zoilite alteration	
C	1152,743	48-16	1-1: WPAR (C)	Low (mbsz)	Host framework texture, cracks, mbsz (self-crushed fragments), trans (carbonate), trans (zoilite), foliated aggregates, isolated mafic carbonates	Quartz, weak W-EX	Restriced within mbsz	Zoilite, overprinted by fine grained carbonates	Predominant	Hydration softening	-	Decrease	Pseudomorphs	Lost	Beneath the D shear zone. Carbonate type overprint zoilite alteration
C	1152,769	48-17	1-1: WPAR (C)	Low (mbsz)	Host framework texture, cracks, mbsz (self-crushed fragments), trans (carbonate), fine grained mafic carbonates	Quartz, weak W-EX	Restriced within mbsz	Rare, overprinted by fine grained carbonates	Common	Hydration softening	-	Decrease	Pseudomorphs	Lost	Beneath the D shear zone. Carbonate type overprint zoilite alteration
C	1153,213	48-23	1-1: WPAR (CZ)	Moderate	Host framework texture, cracks, mbsz (self-crushed fragments), trans (carbonate), zoilite	Quartz, feldspar, weak W-EX	Restriced within mbsz	Rare, overprinted by fine grained carbonates	Rare	Kink band	-	Slightly decrease	Pseudomorphs	Lost	Beneath the D shear zone. Carbonate type WPAR.
C	1154,167	48-33	1-1: WPAR (C)	-	Host framework texture, cracks, mbsz (self-crushed fragments), trans (carbonate), trans (zoilite thin vein)	Quartz, feldspar, weak W-EX	Restriced within mbsz	Rare, overprinted by fine grained carbonates	Rare	Kink band	-	Slightly decrease	Pseudomorphs	Lost	Beneath the D shear zone. Carbonate type WPAR.
C	1155,094	48-50	1-1: WPAR (CZ)	Moderate	Host framework texture, cracks, mbsz (self-crushed fragments), trans (carbonate), trans (zoilite thin vein)	Quartz, weak W-EX, feldspar, weak W-EX	Restriced within mbsz	Zoilite replaced, spots of fine grained carbonate	Common	Kink band	-	Slightly decrease	Pseudomorphs	Lost	Beneath the D shear zone. Between D-E shear zones. Carbonate type WPAR.
C	1155,270	48-54	0-1: WPAR (CZ) (Boundary between Fine/coarse grained granite rocks)	Moderate	Host framework texture, cracks, mbsz (self-crushed fragments), feldspar, calcite	Quartz, weak W-EX, feldspar, weak W-EX	Restriced within mbsz	Zoilite replaced, spots of fine grained carbonate in some grains	Rare	Kink bands in some grains	-	Slightly decrease	Pseudomorphs	Lost	Beneath the D-E shear zones. Between D-E shear zones. Carbonate type WPAR. More feldspars are replaced to zoilite close to mafic carbonates.
C	1156,277	48-70A	1-1: WPAR (CZ)	Moderate	Host framework texture, cracks, mbsz (self-crushed fragments), trans (carbonate), trans (zoilite)	Quartz, feldspar, weak W-EX	Restriced within mbsz	Zoilite, spots of fine grained carbonate	Rare	Kink bands in some grains	-	Slightly decrease	Pseudomorphs	Lost	Beneath the D-E shear zones. Between D-E shear zones. Carbonate type WPAR. Strange crystal growth is observed around zoilite.
C	1156,277	48-70B	1-1: WPAR (CZ)	Moderate	Host framework texture, cracks, mbsz (self-crushed fragments), trans (carbonate), trans (zoilite)	Quartz, feldspar, weak W-EX	Restriced within mbsz	Zoilite, spots of fine grained carbonate in some grains	Rare	Kink bands in some grains	-	Slightly decrease	Pseudomorphs	Lost	Beneath the D-E shear zones. Between D-E shear zones. Carbonate type WPAR. Zoilite was cut the carbonate veins.
C	1156,512	49-1	0-1: WPAR (CZ)	N/C	1. mafic zoilite, self-crushed fragments, calcite	Quartz, weak W-EX + feldspar, weak W-EX	Restriced within mbsz	Zoilite, spots of fine grained carbonate	Rare	Hydration softening	-	Decrease	Pseudomorphs	Lost	Beneath the D-E shear zones. Carbonate type WPAR. More feldspars are replaced to zoilite close to mafic carbonates.
C	1156,785	49-5	0-1: WPAR (CZ)	Low (mbsz)	Host framework texture, cracks, mbsz (self-crushed fragments), calcite	Quartz, weak W-EX, feldspar, weak W-EX	Restriced within mbsz	Zoilite, spots of fine grained carbonate in some grains	Rare	Hydration softening	-	Decrease	Pseudomorphs	Lost	Beneath the D-E shear zones. Carbonate type WPAR. Zoilite (predominant) is cut by carbonate veins.
C	1156,933	49-6	1-1: WPAR (CZ)	Moderate	Host framework texture, cracks, mbsz (self-crushed fragments), zoilite, calcite	Quartz, weak W-EX	Restriced within mbsz	Zoilite, spots of fine grained carbonate in some grains	Rare	Hydration softening	-	Decrease	Pseudomorphs	Lost	Beneath the D-E shear zones. Carbonate type WPAR. Zoilite (predominant) is cut by carbonate veins.

Appendix Results of microtextural observations of fault rocks under the optical microscope.

C	1156923	49-7A	3-3f Ultratextasite (Z)	Random fabric: matrix (ultralime-grains + self-crushed fragments + fine-grained material + small cracks, mbsz) + dark brown fine-grained material + white + self-crushed fragments	Moderate	N/A because of ultralime grain sizes	Predominant	N/A because of ultralime grain sizes	-	-	No pseudomorphs	Lost	
C	1156923	49-7B	3-3f Ultratextasite (Z)	Ultratextasite: matrix (ultralime + self-crushed fragments + fine-grained material + white + self-crushed fragments)	Moderate	N/A because of ultralime grain sizes	Predominant	N/A because of ultralime grain sizes	-	-	No pseudomorphs	Lost	
C	1157354	49-11A	1-1: WPAR (C)	Random fabric: matrix (ultralime-grains + self-crushed fragments + fine-grained material + white + self-crushed fragments)	Moderate (mbsz)	Trans (carbonate), trans (zeolite)	Quartz, feldspar, weak W-EX	Restricted within mbsz	Trans (carbonate), trans (zeolite)	N/A because of ultralime grain sizes	Predominant	Hydration softening	Some spherule carbonate, iron zeolite
C	1157354	49-11B	1-1: WPAR (C/Z)	Host framework texture, cracks, mbsz (self-crushed fragments, hydromica, biotite, kfs, feldspar, weak W-EX)	Moderate (mbsz)	Trans (carbonate), trans (carbonate)	Quartz, feldspar, weak W-EX	Restricted within mbsz	Trans (carbonate), trans (zeolite)	N/A because of ultralime grain sizes	Predominant	Hydration softening	Some spherule carbonate reduced into cracks
C	1158002	49-20	1-1/2 boundary: Calc-silicate	Host framework texture, cracks, mbsz (self-crushed fragments, hydromica, biotite, kfs, feldspar, weak W-EX)	Moderate (boundary mbsz)	No cracks	Quartz, feldspar, W-EX	Predominant	Spots of fine grained carbonates	Spots of fine grained carbonate	Common	Hydration softening	Small numbers of pseudomorphs
C	1160345	49-43	1-1: WPAR (Z)	N/C	Trans (carbonate), trans (zeolite)	Quartz, weak W-EX	Restricted within mbsz	Trans (carbonate), trans (zeolite)	Zoelite in some grains, spots of fine grained carbonates	Common	Hydration softening	In mbsz	
A	1161507	50-4	1-2: WPAR (C/Z)	Moderate (mbsz)	Trans (carbonate), trans (zeolite)	Quartz, weak W-EX	Restricted within mbsz	Trans (carbonate), trans (zeolite)	Change color into grayish white (chlorite?) in some grains	Spherule, iron zeolite	Hydration softening	-	
A	1162366	50-13	1-1: WPAR (C/Z)	High (mbsz)	1. trans (zeolite), trans (carbonate)	Quartz, feldspar, weak W-EX	Restricted within mbsz	1. trans (zeolite), trans (carbonate)	Zoelite in some grains, scattered grains of spherulite	Common	Hydration softening	-	
A	1164048	50-33	1-1: WPAR (Z)	Low (mbsz)	1. trans (zeolite), trans (carbonate)	Quartz, W-EX	Restricted within mbsz	1. trans (zeolite), trans (carbonate)	Zoelite in some grains, scattered grains of spherulite	Common	Hydration softening	Small amounts of fragmented grains in mbsz	
A	1168456	51-31	1-1/4,1 boundary: Ultratextasite (C/Z)	High (mbsz)	Host framework texture, cracks, mbsz (zeolite, small amounts of fine-grained material, white + self-crushed fragments, carbonic, scg)	Quartz, W-EX	Predominant	Quartz, W-EX	N/A due to few residual grains	Common	Hydration softening	-	
A	1170665	52-2	0-1: WPAR (C)	-	Host framework texture, cracks	Quartz, feldspar, weak W-EX	-	Quartz, feldspar, weak W-EX	Spots of fine grained carbonates	Common	Hydration softening	Slightly decrease	
A	1173652	52-31	1-1: WPAR (feldsite vein) (C/Z)	-	Host framework texture, cracks	Quartz, feldspar, weak W-EX	-	Quartz, feldspar, weak W-EX	Replacement of zoelite is predominant, spots of fine grained carbonates	Common	Hydration softening	-	
A	1174648	52-39	1-1: WPAR (C/Z)	High (mbsz)	Host framework texture, cracks, mbsz (zeolite, self-crushed fragments)	Quartz, feldspar, weak W-EX	-	Quartz, feldspar, weak W-EX	Zoelite in some grains	Common	Hydration softening	-	
A	1175459	53-3	1-1: WPAR (C/Z)	-	Host framework texture, cracks	Quartz, feldspar, weak W-EX	-	Quartz, feldspar, weak W-EX	Zeolite in some grains, small amount of sericitic	Common	Hydration softening	-	
A	1179039	53-47	3-3/2,2 boundary: Ultratextasite part (MCC)	High (mbsz)	Random fabric: matrix (ultralime-grains + self-crushed fragments + fine-grained material + white + self-crushed fragments + fine-grained material, rounded, rounded texture + small amounts of folded clay) + clast (self-crushed fragments)	Quartz, weak W-EX	Predominant	Quartz, W-EX	N/A due to few residual grains	Common	Hydration softening	-	
A	1180776	54-8	1-1: WPAR (Z)	Moderate (mbsz)	Trans (zeolite), trans (carbonate)	Quartz, feldspar, weak W-EX	-	Quartz, weak W-EX	Zoelite in some grains, spots of fine grained carbonate, most grains are not altered	Common	Weak hydration softening	-	

Appendix Results of microtextural observations of fault rocks under the optical microscope.

A	1181.854	54-20	1-2; WPAR (CZ)	Host framework texture is barely preserved. Cracks, mbsz (zeolite) matrix + zoicite, aggregates of calcite, fine-grained carbonate matrix with ultrafine-grained zoicite (C).	Quartz, weak W-EX, B-EX, W-EX, feldspar, weak W-EX	Resisted within zeolite mass.	Replacement of zeolite is predominant.	Spherulitic carbonatic, ribbon zoilite	Predominant	Hydration softening	Some spherulitic carbonatic are forced into cracks	Small numbers of deformed pseudomorphs	Between E/F shear zones. Carbonate type WPAR (fresh occurrence, close to host rock). Obsidian, diabase is all present.	Lost	
A	1183.121	54-32	0-1; WPAR (C)	-	Host framework texture, cracks, mbsz (feldsp., sc.-crushed fragments.)	Trans (carbonate), trans (zoicite)	Trans (carbonate)	Ribbon zoilite, Ribbon carbonatic	Small amounts	-	-	Almost no decrease	Decrease	Decrease	Decrease
A	1183.306	54-35	2-1; WPAR (CZ) (with veins filled with self-crushed fragments)	Host framework texture, cracks, mbsz (self-crushed fragments (with fragmented boulders), calcite).	Trans (carbonate), trans (zoicite)	Quartz, feldspar, weak W-EX	Restricted within mbsz	Zoilite, Spots of fine grained carbonatic	Common	Hydration softening	-	Decrease	Pseudomorphs	Lost	
A	1183.764	54-39	2-2; Fault breccia (C) (hydraulic brecciation with carbonate matrix)	Random fabric, matrix (fine-grained self-crushed Fragments + fine-grained zoilite + clast (self-crushed carbonate) + carbonate aggregates, carbonate hydraulic brecciation texture, cracks).	Trans (carbonate)	Quartz, feldspar, weak W-EX	Predominant zoilite	Spherulitic carbonatic, ribbon zoilite	Predominant	Hydration softening	Extremely decrease	Small numbers of pseudomorphs	Abundant horizontal veins are altered to pseudomorphs	Abundant horizontal veins are altered to pseudomorphs	
A	1183.645	55-10	0-1; WPAR (CZ)	-	Host framework texture, cracks, Trans (zoicite), trans (thin veins of carbonatic).	Quartz, feldspar, weak W-EX	Carbonatic spots in some veins.	Ribbon carbonatic	Small amounts	-	-	No decrease	Pseudomorphs	Upper part of F shear zone. Carbonate type fault breccia zone. Hydraulic brecciation texture with carbonate matrix overprints fault breccia with zoilite matrix.	Upper part of F shear zone. Carbonate type fault breccia zone. Hydraulic brecciation texture with carbonate matrix overprints fault breccia with zoilite matrix.
A	1186.478	55-22	2-2; Fault breccia (Z)	Moderate	Random fabric, matrix (fine-grained self-crushed Fragments + fine-grained zoilite + clast (self-crushed carbonate) + carbonate aggregates, carbonate hydraulic brecciation, cracks).	Trans (zoicite), trans (carbonate)	Predominant	Zoilite, Subporphyroblasts (formed in some class, cleat-spacer weak W-EX)	Change color into greyish white (chloritization?)	Predominant	Hydration softening	Extremely decrease	One grain of deformed pseudomorphs	Middle part of F shear zone. Zoilite type fault breccia. Feldspars are replaced by secondary stilpnomelane (?)	Lost
A	1187.488	55-29	2-2; Fault breccia (C)	High	Random fabric, matrix (fine-grained self-crushed Fragments + fine-grained zoilite + clast (self-crushed carbonate) + carbonate aggregates, carbonate hydraulic brecciation, cracks).	Trans (carbonate), subgrains are forced in some grains.	Predominant	Zoilite, Spots of fine grained carbonatic	Spherulitic carbonatic	Predominant	Hydration softening	Extremely decrease	Small numbers of pseudomorphs	Some hydrated spherulites are released into cracks	Some hydrated spherulites are released into cracks
						Quartz, W-EX, feldspar, weak W-EX								Middle part of F shear zone. Carbonate type fault breccia.	

淡路島、野島平林 NIED 掘削コアの 1,140m 深度破碎帶における精密断層岩分布解析

田中秀実^{*1}・松田達生^{*2}・小村健太朗^{*2}・池田隆司^{*2}
小林健太^{*3}、島田耕史^{*4}、新井崇史^{*5}
富田倫明^{*6}、平野 聰^{*7}

^{*1}愛媛大学

^{*2}防災科学技術研究所

^{*3}新潟大学

^{*4}早稲田大学

^{*5}信州大学

^{*6}筑波大学

^{*7}海洋科学技術センター

要 旨

兵庫県南部地震（1995, M=7.2）に伴い、淡路島北西部に地震断層（野島断層）が出現した。科学技術庁防災科学技術研究所では、野島平林において断層貫通掘削を実施し（掘削深度 1,822 m), 1,140 m, 1,300 m, および 1,789 m の 3 深度の破碎帶を含むコアを回収した。本論文では、1,140 m 破碎帶の断層岩分布様式、およびそれらの微小構造の観察結果を記載している。これらの解析を通して、次の諸点が明らかとなった。(1)掘削深度 1,140 m において、野島断層の破碎帶の幅は 70 m 以上となっており、6 つ剪断帯（A～F 帯）を含んでいる。(2) D 帯は 12.1 m の幅を持ち、中軸部の D₂ 亜帯に薄いシードタキライト様の岩石を挟むことから、主要なすべり面は D₂ 亜帯の基底面（掘削深度 1,141.24 m）である可能性が高い。(3) A～F の各剪断帯に共通する特徴として、中軸部のウルトラカタクレーサイト/シードタキライト帯に水酸化鉄/苦鉄質炭酸塩型の変質作用が認められ、その上盤、下盤側に、炭酸塩、沸石に富む水圧破碎組織が、それぞれ認められることが挙げられる。上盤の変質作用は、CO₂ を溶存した表層水が、下盤は Na⁺ に富む流体が、それぞれ深く関与し、間震期（interseismic period）に岩石-水反応を起こした結果、形成されたものであると考えられる。また、水圧破碎組織は、地震発生時に超静水圧（super hydrostatic）状態が発生したことを示唆している。中軸部のウルトラカタクレーサイト/シードタキライト帯は、地震時に大変位をもたらした摩擦発熱帯（friction/heat generation zone）である可能性が高い。一方、この帯は、上盤と下盤の岩石-水反応を隔離していることから、間震期においては、流体のバリアとして機能していたものと考えられる。

キーワード：兵庫県南部地震、野島断層、断層岩分布、変形・変質微小構造